


















Brief Communication

FLOURY ENDOSPERM20 encoding SHMT4 is required for rice endosperm development

Mengyuan Yan^{1,†} , Tian Pan^{2,†} , Yun Zhu^{1,†} , Xiaokang Jiang², Mingzhou Yu² , Rongqi Wang², Feng Zhang¹ , Sheng Luo¹ , Xiu hao Bao² , Yu Chen¹ , Binglei Zhang^{1,2} , Ruonan Jing² , Zhijun Cheng¹ , Xin Zhang¹ , Cailin Lei¹ , Qibing Lin¹ , Shanshan Zhu¹ , Xiuping Guo¹, Yulong Ren^{1,*}  and Jianmin Wan^{1,2,*} 

¹National Key Facility for Crop Gene Resources and Genetic Improvement, Institute of Crop Sciences, Chinese Academy of Agricultural Sciences, Beijing, China

²State Key Laboratory for Crop Genetics and Germplasm Enhancement, Jiangsu Plant Gene Engineering Research Center, Nanjing Agricultural University, Nanjing, China

Received 14 January 2022;

revised 12 May 2022;

accepted 16 May 2022.

*Correspondence (Tel +861082105523; fax +861082105523; emails renyulong@caas.cn; Tel +861082105523; fax +861082105523; wanjianmin@caas.cn)

†These authors contributed equally to this work.

Keywords: rice, endosperm development, SHMT, SAMS2, methylation.

Endosperm stores starch and proteins in cereal crop seeds, providing a major calorie source for human consumption. Rice, given its agricultural importance and rich genetic resources, serves as a model crop for dissecting the molecular basis of endosperm development. Although many genes affecting endosperm development have been functionally characterized, our understanding of storage substance accumulation remains fragmented (He *et al.*, 2021; Huang *et al.*, 2021). Serine hydroxymethyltransferases (SHMTs) catalyse the reversible conversion of glycine to serine in known organisms, including plants (Schirch and Szebenyi, 2005). Genetic evidence from plants suggests the involvement of SHMTs in biotic and/or abiotic stress responses (Liu *et al.*, 2012; Moreno *et al.*, 2005), but their potential functions in endosperm development remain obscure.

To dissect the molecular mechanisms underlying endosperm development, we identified seven allelic *floury endosperm* mutants *flo20-1* to *flo20-7* from an ethylmethanesulfonate-mutagenized pool of *japonica* rice variety Kitaake (Figure S1) and chose *flo20-1* for in-depth studies. *flo20-1* plants displayed defective endosperm development, as evidenced by floury endosperm appearance and ~23% reduction in 1000-grain weight at maturity (Figure 1a,b). Starch and protein contents were reduced but lipid content was increased in *flo20-1*, compared with wild type (WT; Figure 1b). To investigate the cytological basis of disrupted storage substance accumulation, we performed scanning electron microscopy (SEM) and light microscopy of endosperm. *flo20-1* endosperm was filled with loosely arranged and abnormal starch granules (SGs), compared with tightly packed and sharp-edged SGs in WT (Figure 1c). Coomassie blue staining of developing endosperm at 10 days after flowering (DAF) revealed two types of protein bodies (PBs): lightly stained PBIs and densely stained PBII in WT (Figure 1d). Notably, PBII morphology appeared to be amorphous in *flo20-1*

(Figure 1d), which is similar to a reported mutant with altered storage protein composition (Ashida *et al.*, 2011). Floury grains from reciprocal cross plants phenocopied *flo20-1* (Figure S2), suggesting that *FLO20* directly regulates endosperm development.

Map-based cloning combined with sequencing revealed that each *flo20* mutant harbours a single-nucleotide substitution in *Os01g0874900*, causing mis-sense, non-sense or splicing mutations (Figures 1e and S3). We introduced genomic or GFP-fused *Os01g0874900* into *flo20-1* calli to generate transgenic plants for complementation. As predicted, *flo20-1* carrying either transgene displayed translucent endosperm (Figure 1f), confirming that *Os01g0874900* represents *FLO20* and that *FLO20*-GFP was functional. *FLO20* encodes a predicted 64.8-kDa protein harbouring an SHMT domain (<https://www.uniprot.org/uniprot/Q8RYY6>), named SHMT4. Immunoblotting using anti-SHMT4 antibodies detected SHMT4 in all tissues examined. SHMT4 levels were lower during early endosperm development, peaked at ~12 DAF and decreased thereafter (Figure 1g). SHMT4-GFP localized to nuclei in developing endosperm (Figure 1h).

Given that SHMT4 contains an SHMT domain, we determined whether *SHMT4* loss affected the SHMT enzymatic activity, and found that more than 64% of SHMT activity was abolished in *flo20-1* (Figure 1i). Unexpectedly, we failed to detect the SHMT4 activity *in vitro* (Figures 1j and S4). SHMTs usually function as homozygous or heterozygous complexes (Anderson *et al.*, 2012; Schirch and Szebenyi, 2005). As anticipated, we verified SHMT4's interacting with itself and two homologues SHMT3&5 using a combination of *in vitro* yeast two-hybrid (Y2H) as well as *in vivo* biomolecular fluorescence complementation (BiFC) and co-immunoprecipitation assays (Figures 1k–m and S5). Using high-performance liquid chromatography, we detected the SHMT enzymatic activity of SHMT4-GFP precipitate (Figure 1n), suggesting that SHMT4 may cooperate with other proteins to execute SHMT function. We indeed detected the SHMT activity of SHMT3 alone *in vitro* (Figures 1o and S6) and found that *SHMT3* mutation slightly but significantly compromised SHMT activities of SHMT4-GST precipitate (Figures 1p and S7). Consistently, the *SHMT3* knockout mutant exhibited a 35.3% reduction in SHMT activity, compared with a 64.1% reduction in *flo20-1*, although *SHMT3* loss did not obviously affect endosperm development (Figures 1i and S8). Together, these results suggested that SHMT4 works cooperatively with other proteins such as SHMT3 to execute SHMT activity, in which SHMT4 may be more important than SHMT3.

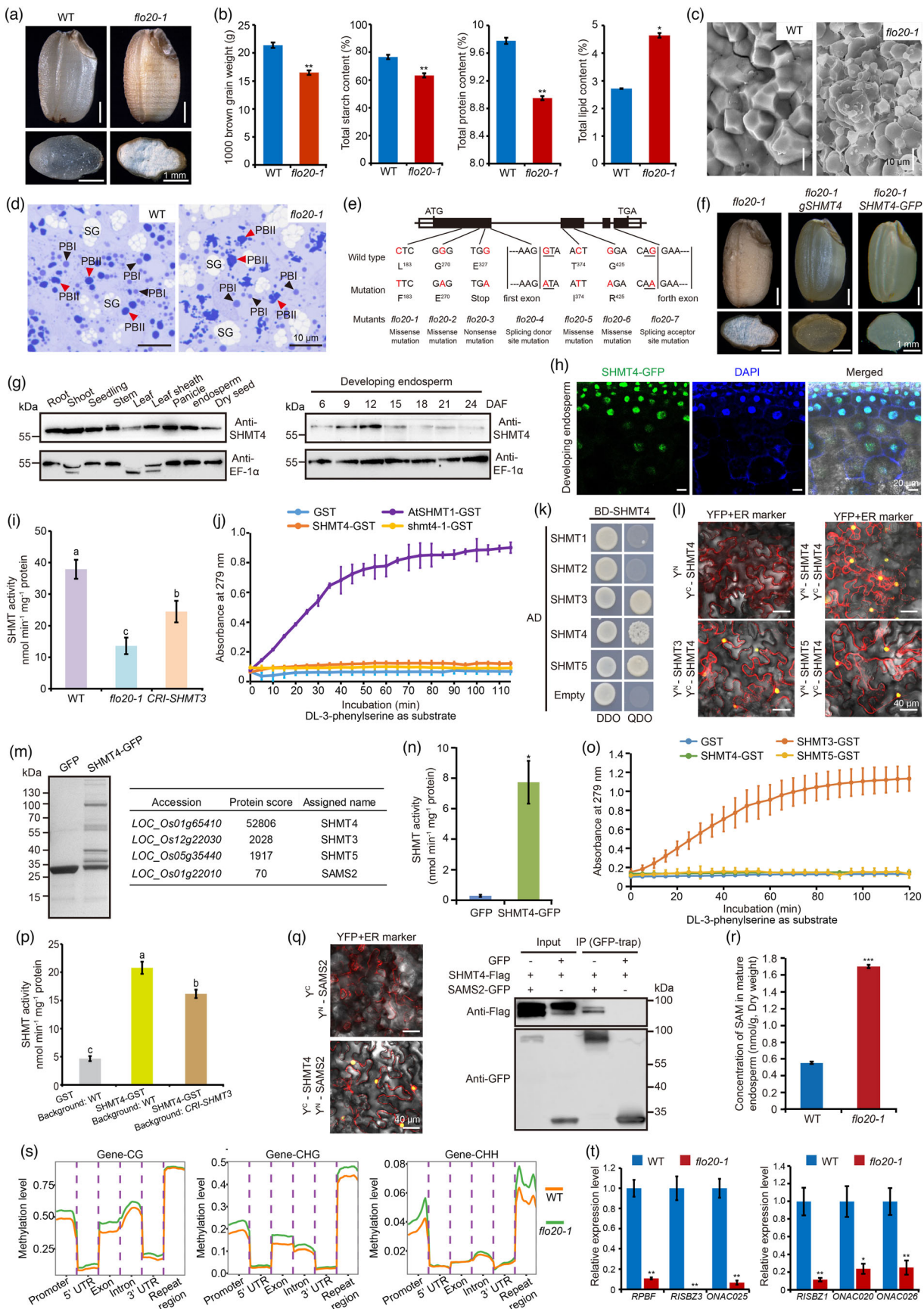


Figure 1 SHMT4 is required for rice endosperm development. (a) Full view and transverse sections of WT and *flo20-1* seeds. (b–d) 1000-brown kernel weight and physicochemical characteristics (b), SEM (c) and light microscopy (d) of WT and *flo20-1*. (e) Gene structure of *SHMT4* and mutation sites of *flo20* alleles. Mutated nucleotides are shown in red. Putative splicing sites are underlined. (f) Complementation tests of *flo20-1* grains. (g) Expression patterns of SHMT4. (h) Subcellular localization of SHMT4-GFP. (i) Total SHMT activities in WT, *flo20-1* and *CRI-SHMT3* mutants. (j) The activity analysis of SHMT4 *in vitro*. (k–l) Y2H (k) and BiFC assay in tobacco (l) showing the interactions of SHMT4 and its homologues. (m) Summary of proteins co-precipitated with SHMT4-GFP, as identified by mass spectrometry. (n) The SHMT activity assay in SHMT4-GFP and GFP transgenic rice. (o) Enzymatic activity of SHMT3&5 *in vitro*. (p) SHMT activity of SHMT4-GST precipitate prepared from different background rice. (q) Verification of SHMT4 interacting with SAMS2 using BiFC and Co-IP assays. (r) Measurement of SAM concentration in WT and *flo20-1*. (s) Global distribution of DNA methylation levels over promoter, exon, intron and UTR of genes as well as repeat region. (t) RT-qPCR analysis of *RPBF*, *RISBZ3*, *ONAC025*, *RISBZ1*, *ONAC020* and *ONAC026* in WT and *flo20-1* endosperm at 10 DAF. Values given are means \pm SD. Columns with different letters indicate significant differences ($P < 0.05$). Throughout, $*P < 0.05$, $**P < 0.01$, $***P < 0.001$ by Student's *t*-test.

We specifically detected the *S*-adenosyl-L-methionine synthetase SAMS2 in the SHMT4-GFP precipitate by mass spectrometry (Figure 1m), and confirmed SHMT4's interaction with SAMS2 via BiFC and co-immunoprecipitation assays in tobacco (Figure 1q). SAMSs catalyse the conversion of methionine to produce SAM, which serves as the methylation donor in transmethylation reactions and an intermediate in polyamine and ethylene biosynthesis (Li *et al.*, 2011). We measured SAM concentrations in WT and *flo20-1* endosperm, finding that SAM level was threefold higher in *flo20-1* (Figure 1r). We next performed bisulphite sequencing of WT and *flo20-1* endosperm DNA to determine whether *SHMT4* loss affects genome-wide DNA methylation (Table S1). Compared with WT, CG, CHG and CHH methylations were higher in *flo20-1* (Figure 1s, Table S2), suggesting a possible role of SHMT4 in endosperm DNA methylation. Differentially methylated regions (DMRs) analysis identified 25 715 DMRs and 15 888 differentially methylated genes (DMGs) between WT and *flo20-1* (Table S3, Data S1), which included genes involved in storage substance biosynthesis, transport or accumulation (Table S4). Additionally, expression levels of several transcript factor genes required for starch and protein accumulation were significantly reduced in *flo20-1* (Figure 1t). Together, the *SHMT4* mutation causes genome-wide methylation changes in developing endosperm, probably through affecting SAM production.

A leaky *SHMT4* allele was recently reported to confer enhanced cadmium tolerance and selenium accumulation by affecting their uptake and assimilation in root and/or shoot (Chen *et al.*, 2020). However, the putative SHMT4 function in endosperm development remains unclear. Here, we identified seven allelic *SHMT4* mutants defective in endosperm development. Storage protein composition greatly determines nutritional and functional qualities of cereal crops. We noted that *SHMT4* loss caused a disruption in storage protein composition, suggesting the potential value of *SHMT4* in breeding rice with special demands. Together, our study provided a functional link between SHMT proteins and endosperm development in plants.

Acknowledgements

This work was supported by National Key R&D Program of China (2021YFF1000200) and Central Public-Interest Scientific Institution Basal Research Fund, China (Y2021YJ18).

Conflicts of interest

The authors declare no conflict of interest.

Author contributions

J.M.W. and Y.L.R supervised the project. M.Y.Y, T.P., Y.L.R., Y.Z., X.K.J. and M.Z.Y. performed the experiments. Other authors provided technical supports; Y.L.R and M.Y.Y prepared the manuscript.

References

- Anderson, D.D., Woeller, C.F., Chiang, E.P., Shane, B. and Stover, P.J. (2012) Serine hydroxymethyltransferase anchors *de novo* thymidylate synthesis pathway to nuclear lamina for DNA synthesis. *J. Biol. Chem.* **287**, 7051–7062.
- Ashida, K., Saito, Y., Masumura, T. and Iida, S. (2011) Ultrastructure of protein bodies in mutant rice (*Oryza sativa* L.) with altered storage protein composition. *Breeding Sci.* **61**, 201–207.
- Chen, J., Huang, X.Y., Salt, D.E. and Zhao, F.J. (2020) Mutation in *OsCADT1* enhances cadmium tolerance and enriches selenium in rice grain. *New Phytol.* **226**, 838–850.
- He, W., Wang, L., Lin, Q.L. and Yu, F. (2021) Rice seed storage proteins: biosynthetic pathways and the effects of environmental factors. *J. Integr. Plant Biol.* **63**, 1999–2019.
- Huang, L.C., Tan, H.Y., Zhang, C.Q., Li, Q.F. *et al.* (2021) Starch biosynthesis in cereal endosperms: an updated review over the last decade. *Plant Commun.* **2**, 100237.
- Li, W.X., Han, Y.Y., Tao, F. and Chong, K. (2011) Knockdown of SAMS genes encoding *S*-adenosyl-L-methionine synthetases causes methylation alterations of DNAs and histones and leads to late flowering in rice. *J. Plant Physiol.* **168**, 1837–1843.
- Liu, S.M., Kandoth, P.K., Warren, S.D., Yeckel, G. *et al.* (2012) A soybean cyst nematode resistance gene points to a new mechanism of plant resistance to pathogens. *Nature*, **492**, 256–260.
- Moreno, J.I., Martin, R. and Castresana, C. (2005) Arabidopsis SHMT1, a serine hydroxymethyltransferase that functions in the photorespiratory pathway influences resistance to biotic and abiotic stress. *Plant J.* **41**, 451–463.
- Schirch, V. and Szebenyi, D.M. (2005) Serine hydroxymethyltransferase revisited. *Curr. Opin. Chem. Biol.* **9**, 482–487.

Supporting information

Additional supporting information may be found online in the Supporting Information section at the end of the article.

Data S1 List of DMRs between WT and *flo20-1* endosperm.

Figure S1–S8 Supplementary Figures.

Table S1–S4 Supplementary Tables.